Journal of Metals, Materials and Minerals. Vol.16 No.2 pp.1-6, 2006

Effect of Decarburization on Microstructure of DC-Plasma Nitrided H 13 Tool Steel

Patama VISUTTIPITUKUL[1*], Chuleeporn PAA-RAI[2] and Kuwahara HIDEYUKI [3]

[1]Department of Metallurgical Engineering, Chulalongkorn University, Bangkok 10330,Thailand.
[2]Graduated School of Engineering, Department of Metallurgical Engineering
Chulalongkorn University, Bangkok 10330, Thailand.
[3]Research Institute for Applied Sciences, Kyoto 606-8201, Japan.

Received Aug. 31, 2006
Accepted Oct. 30, 2006

Abstract

Decarburization may occur during heat treatment of H13 steel resulting in carbon deficiency near the specimen surface. Microstructures and properties of H13 tool steel after surface treatment such as plasma nitriding can be affected by decarburization. This study is focused on the microstructure of plasma nitrided H13 steel. Decarburized and non-decarburized H13 steel was plasma nitrided for 36-72 ks at temperatures varying from 773 to 823 K. The microstructure of the plasma nitrided layer was analyzed by an optical microscope and Electron Probe Micro Analysis (EPMA). The thickness of the nitriding layer is measured. The microstructures of the decarburized and the non-decarburized and plasma nitrided samples are different. The non-decarburized sample shows only one surface layer which consists of Fe_3N (ε), Fe_4N (γ′), and CrN phases. In contrast, the nitriding layer of the decarburized sample consists of two layers. The top layer adjacent to the surface contains only Fe_3N (ε) and Fe_4N (γ′) phases, while the beneath layer consists of Fe_3N (ε), Fe_4N (γ′), and CrN phases. The difference of microstructures also affects surface hardness and hardness depth. Surface hardness and hardness depth of the decarburized samples is lower than that of the non-decarburized samples.

Key words : Plasma nitriding, Decarburization, H13 tool steel, CrN precipitate

Introduction

H 13 tool steel has been used in many applications such as die-casting dies, extrusion dies and forging dies due to its unique properties: high hardenability, low amount of dimensional change, high strength and ductility, good tempering resistance and moderate cost. The applications of H13 tool steel, however, are limited by low hardness and wear resistance.[1-3] In order to increase the hardness and wear resistance, H13 tool steel must be heat treated and quenched to transform the matrix to the martensite phase followed by surface treatments. Plasma nitriding is one of the surface treatment methods applied to heat treat H13 tool steel to achieve high surface hardness by nitride precipitates in the nitriding layer.[4-5]

During heat treatment without controlled atmosphere, decarburizing might occur at the surface of specimens resulting in inhomogeneous carbon content in the specimens. This inhomogeneous carbon content affects hardenability, microstructure and also the hardness of steel after heat treatment. A low carbon content of an alloy decreases the hardenability of the alloy. The decarburized area has a low carbon content and consists of a ferrite phase; consequently, ferrite still exists in the low carbon content area along the specimen surface and, hence, the hardness of the surface area is lower than that in the beneath layer.[4,6] The difference of microstructure prior to plasma nitriding causes the difference in microstructures of the nitrided specimen; which may influence the mechanical properties of the H13 tool steel. In this experiment, the effect of decarburization on microstructures and phases that existed in the nitriding layer and hardness of plasma nitrided H13 tool steel was studied.

Phone +66-2218-6947, Fax. +66-2218-6942, E-mail:Patama.V@chula.ac.th
Phone +66-2218-6947, Fax. +66-2218-6942, E-mail:chuleeporn_p@hotmail.com
Phone +81-75-705-1092, Fax. +81-75-701-1217, E-mail: kuwahara@rias.or.jp

Experimental Procedure

Material

In this experiment, H 13 tool steel rods with 18 mm. in diameter were used as material to be nitrided. The chemical composition of the H13 tool steel was analyzed by the Spark Emission Spectrometer and was shown in Table 1.

Table 1. Chemical composition of H13 tool steel.

Elements	Fe	C	Si	Mn	P	S	Cr	Mo	V
H13 Sample	Balance	0.35	1.10	0.40	0.02	0.02	5.10	1.14	0.96
AISI H13 steel	Balance	0.32 - 0.45	0.80 - 1.25	0.20 - 0.60	0.03 max	0.03 max	4.75 - 5.50	1.10 - 1.75	0.80 - 1.20

Sample Preparation

The samples were divided into 2 groups. Both groups were prepared from the cylindrical rod of AISI H13 steel with a diameter of 18 mm. The samples in the first group were cut into a cylindrical-shape with a height of 10 mm prior to heat treatment. The samples in the second group were heat treated as a cylinder rod before cutting into a cylindrical-shape with a height of 10 mm. For the samples of the second group, the sample at rod ends will not be used in order to eliminate the effect of decarburizing. All of the samples, in both groups, were heat treated by austenitizing at 1273 K for 2.4 ks in an ambient atmosphere and quenching in quenching oil to room temperature followed by tempering at 773 K for 3.6 ks. Before plasma nitriding the samples were ground by SiC paper and polished, with a final lap using 0.5 μm alumina powder.

Plasma Nitriding

All samples were cleaned in acetone by an ultrasonic cleaning machine for 600 seconds prior to plasma nitriding. The plasma nitriding chamber was evacuated by a mechanical booster pump until the gas pressure reached 0.013 Pa in order to keep the partial pressure of oxygen and moisture as low as possible. The DC glow discharge of hydrogen was ignited and then the samples were heated up to the nitriding temperature. After the sample temperature reached the nitriding temperature, nitrogen gas was introduced into the nitriding chamber, at which the plasma nitriding process started. The treatment was done under a N_2+H_2 atmosphere with a H_2:N_2 ratio of 3:1 by pressure. The nitriding holding times were varied from 36-72 ks. The applied bias voltage was 200 V with a direct current of 0.1 A. The nitriding temperatures in this study were 773 and 823 K. Table. 2 summarized the nitriding conditions. Figure 1 shows the illustration of the nitriding apparatus.

Table 2. Plasma nitriding conditions

Temperature (K)	Time (ks)	H2:N2 ratio	Voltage (V)	Current (A)
773	36	3:1	200	0.1
	72			
823	36			
	72			

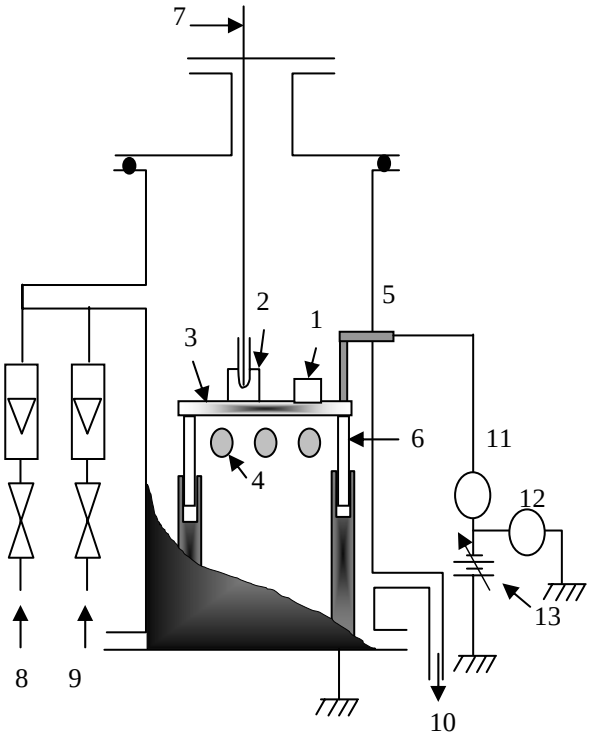

(1) Specimen, (2) Dummy specimen,
(3) Specimen table,
(4) Heater in quartz tube,
(5) Cathode, (6) Insulator,
(7) Thermocouple, (8) Nitrogen gas inlet, (9) Hydrogen gas inlet, (10) To Mechanical booster and rotary pump,
(11) Ampere Meter, (12) Voltage meter,
(13)DC power supply

Figure 1. Nitriding apparatus

Characterization

In order to identify the phases existing in the nitriding layer, all samples were analyzed with a Glancing Incident angle X-ray Diffractometer (GIXD) at an incident angle of 1º and 5º and an X-ray Diffractometer (XRD). The microstructures of the nitrided samples were observed with an optical microscope.Both decarburized and non decarburized samples were qualitatively analyzed by using Electron Probe Microanalysis (EPMA) to map the element content in the nitriding layer. Micro-Vicker hardness testing was employed to measure the surface hardness and its profiles in the cross-section of specimens with a load of 50 g.

Results and Discussions

Microstructures of Nitriding Layer

Figure 2 shows the microstructure of non-decarburized samples after plasma nitriding at 773-823 K for 7.2-14.4 ks. The nitriding layer in Figure 2 is a dark grey colored layer with some precipitates which will be discussed in the following section. The thickness of an nitriding layer an increases with increase of either nitriding time or nitriding temperature, as shown in Table 3, since the growth of nitriding layer in plasma nitriding is controlled by the diffusion process as reported by many research groups. The microstructures of decarburized samples after plasma nitriding at 773-823 K for 7.2-14.4 ks are shown in Figure 3. Effect of the nitriding time and the nitriding temperature on the thickness of nitriding layer of decarburized samples is similar to that of non decarburized samples as seen in Table 3. The thickness of nitriding layer increases with increasing the nitriding time and nitriding temperature as expected because the diffusion of nitrogen atoms controlled the growth of the nitriding layer as that of the non-decarburizing sample. However, the growth rate of decarburized samples differs from that of non-decarburized samples due to the effect of carbon content.

Table 3. Thickness of nitriding layer.

Temperature (K)	Time (ks)	Layer thickness (μm)	
		Decarburized	Non-decarburized
773	36	88.06	96.01
	72	91.71	113.61
823	36	118.89	129.94
	72	169.89	173.09

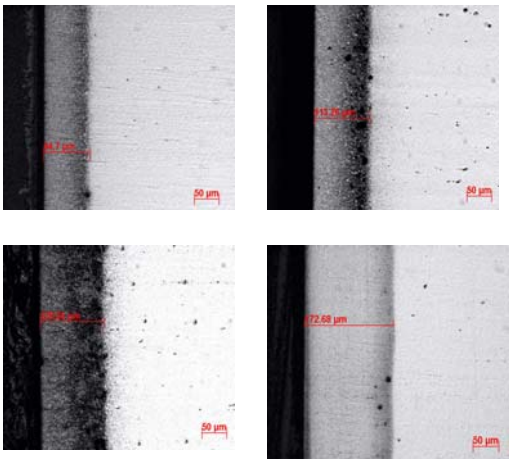

Figure 2. Cross-sectional microstructure of non-decarburized samples plasma nitriding at (a) 773 K for 36 ks, (b) 823 K for 36 ks, (c) 773 K for 72 ks and d) 823 K for 72 ks

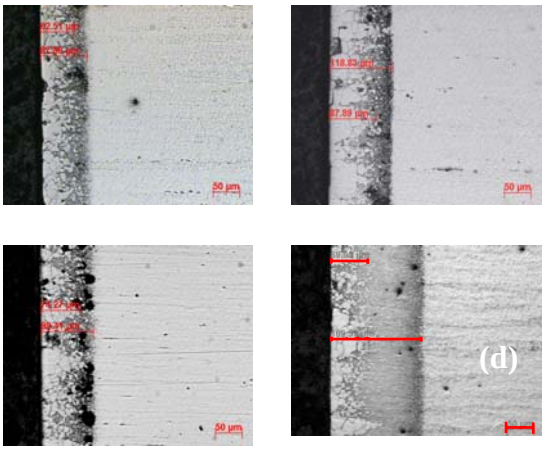

Figure 3. Cross-sectional microstructure of decarburized Samples plasma nitriding at a) 773 K for 36 ks, b) 823 K for 36 ks, c) 773 K for 72 ks and d) 823 K for 72 ks

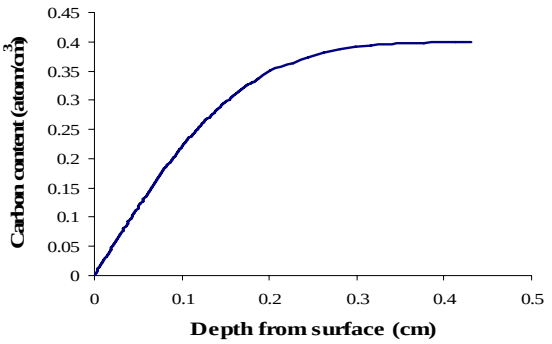

Figure 4. Calculation of carbon concentration profile in decarburized sample

The microstructure of the decarburized samples shows that the nitriding layer in decarburized samples consists of two layers indicated by a different color: a white color layer and a dark grey color layer. The white color layer locates on the top surface of decarburized and plasma nitrided sample, in contrast the dark grey color layer lies beneath the white color layer and is adjacent to the matrix. The difference of microstructure in Figure 2 and Figure 3 is because of a different carbon content at the surface due to decarburization reactions during heat treatment in Equation 1. The concentration profile of carbon in the decarburized sample can be calculated from Equation 2 by assuming that the carbon equivalent in air is equal to zero percent.

$C\gamma + CO2 = 2CO$ Equation 1

$$C(x,t) = C_s - (C_s - C_0)erf\left(\frac{x}{2\sqrt{Dt}}\right)$$ Equation 2

where, C is carbon concentration, Cs is carbon concentration at the surface, C_0 is carbon concentration in the iron matrix, x is distance from surface, Figure 4. D is diffusion coefficient, and t is decarburizing time.[4,7]

Characterization of Nitriding Layer

After plasma nitriding, the non-decarburized samples are examined by GIXD at the incident angle of 1 and 5 degrees and XRD. It is seen that the nitriding layer consisted of Fe_3N (ε), Fe_4N (γ′), and CrN phases as shown in Figure 5. The relative intensity of each peak varies with the incident angle of GIXD. This shows that the volume fraction of each phase is different depending on the depth from the surface. By assuming that at the penetration depth X-ray intensity is 0.0001 of the incident x-ray intensity, X-ray penetration depth from calculations are 25.2 μm, 125.6 μm and 1250 μm into iron matrix for GIXD at the incident angle of 1˚, 5˚ and XRD respectively. It is found that the volume fraction of Fe_3N and Fe_4N increases along the depth direction from the surface. On the contrary, the volume fraction of CrN phase, described by the CrN peaks at 2θ = 41.6, continuously increases in the depth Figure 6.

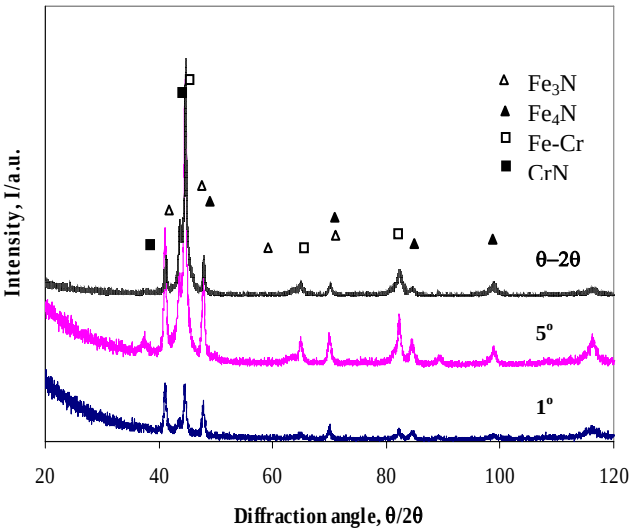

plasma nitrided sample at 823 K for 72 ks

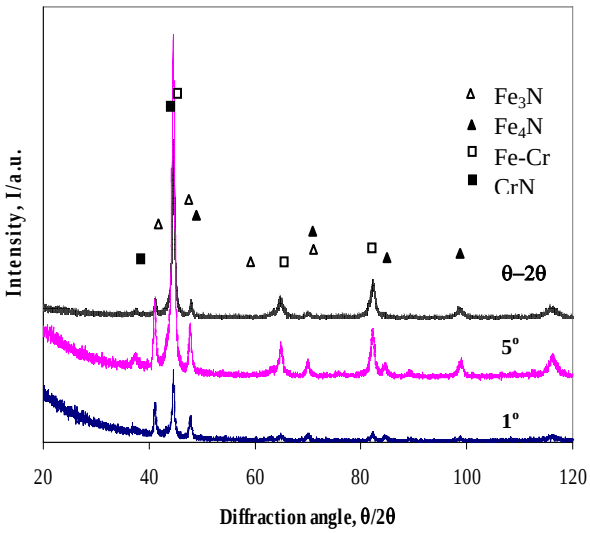

Figure 6. GIXD at the incident angle of 1 degree and 5 degree and XRD profiles of decarburized plasma nitrided sample at 823 K for 72 ks

GIXD and XRD profiles of decarburized samples after plasma nitriding show that the nitriding layer consists of Fe_3N (ε) and Fe_4N (γ′). In GIXD at the incident angle of 5° and XRD profiles, a low intensity peak of CrN is detected at 38.8° while no CrN peak is detected in GIXD profile at the 1° incident angle. This means that a small amount of CrN existed in the nitriding layer at the depth from surface greater than 125.6 μm.

The difference of microstructures of the nitriding layer in the first and second group as shown in Figure 2 and Figure 3 can be explained

by different chemical compositions and different phases in the nitriding layer. For the non-decarburized samples, there is only one dark grey layer which is consisted of Fe_3N (ε), Fe_4N (γ′), and CrN in the entire layer. On the other hand, the microstructure of decarburized and plasma nitriding sample is composed of two layers: white color and dark grey color. From EPMA analysis, the white color layer is the decarburized zone as shown by low concentration of carbon in this layer in Figure 7(a), compared to EPMA analysis of non-decarburized, and plasma nitrided sample in Figure 7 (b). Since this layer has a low carbon concentration, chromium carbide would not precipitate. Therefore, there is a large amount of dissolved chromium in the matrix resulting in increasing corrosion resistance in this area as can be seen as the white-color layer on the top surface. There is no CrN precipitated in this white-color layer as shown by the profile of GIXD at 1ºincident angle while there are CrN precipitates homogenously distributed in the nitriding layer of non-decarburized sample as shown by high intensity peaks of CrN in all GIXD profiles. EPMA analysis of the particles in Figure 7 shows that the particles have a high amount of carbon, nitrogen and chromium. According to GIXD and XRD results, the particles are chromium carbide and chromium nitride. It is seen that chromium carbide and chromium nitride coexists in the nitriding layer of both non-decarburized and decarburized samples as shown in Figure 7 (a) and (b) respectively. The conclusion from this result is that, in decarburized sample, there is no CrN precipitate in the white-color layer because it lacks of chromium carbide due to a low percentage of carbon. The different microstructures should have different properties such as hardness and so on.

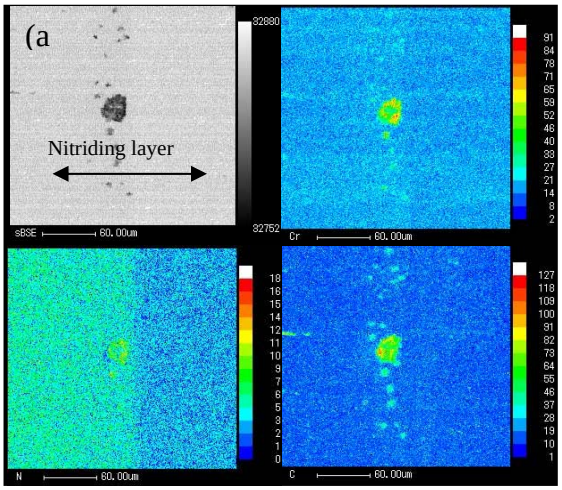

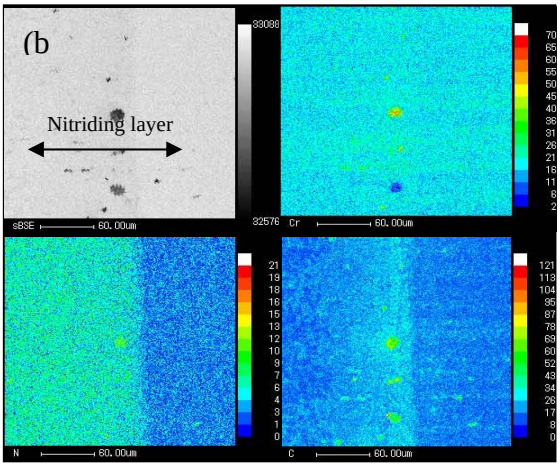

Figure 7. EPMA mapping results of specimen plasma nitrided at 823 K for 72 ks ; (a) non-decarburized sample (b) decarburized sample

Hardness Measurement

The hardness of all plasma nitrided samples increases by up to more than 1000 HV as shown in Figure 8. The increase of hardness infers that the wear resistance of plasma nitrided H13 tool steel should increase. Decarburizing occurred during heat treatment affects the hardness of plasma nitrided samples. The decarburized samples tend to have lower surface hardness as well as hardness depth as seen from the hardness profiles. Normally the increase of hardness in the nitriding of iron is governed by precipitation hardening, therefore, the decarburized samples have lower surface hardness and hardness depth since it contains a lower amount of CrN precipitates in the nitriding layer.

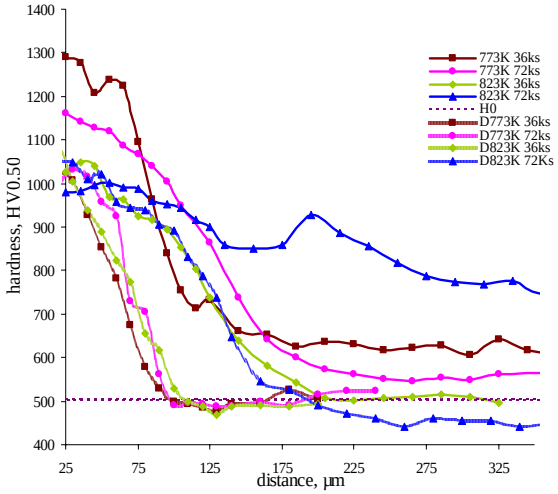

Figure 8. Hardness profiles of decarburized and non-decarburized samples

Conclusion

1. The difference of carbon concentration at surface due to decarburizing affects on nitriding microstructure of H13 tool steel.

2. The nitriding surface of decarburizing samples has two layers. There is Fe_3N (ε) and Fe_4N (γ′) precipitates in the top surface layer of nitriding samples. The beneath layer adjacent to the matrix, consists of Fe_3N (ε), Fe_4N (γ′), and CrN.

3. The non-decarburizing sample shows only one layer. The entire nitriding layer consists of Fe_3N (ε), Fe_4N (γ′), and CrN

4. Surface hardness is remarkably increased by plasma nitriding due to the formation of nitride precipitates. The decarburized samples tend to have lower hardness and hardness depth than that of non-decarburized samples.

References

1. Smith Willium F. 1993. *Structure and Properties of Engineering Alloys.* 2nd edition, New York : McGraw Hill :405-409, 599.

2. Miola, E. J., de Souza, S. D., Olzon-Dionysio, M., Spinelli, D., dos Santos, C.A. 1999. *Surf. Coat. Technol.* **116-119** : 347-351.

3. ASM International, 1990. *ASM Metal Handbook.* Vol. 1. Materials Park, OH : ASM Internation : 439-444.

4. Brooks, Charlie R. 1992. *Principles of the Surface Treatment of Steels.* New York : Technomic Publishing : 182-190.

5. Pye, David. 2003. *Practical Nitriding and Ferritic Nitrocarburizing*. Materials Park, OH : ASM International : 65-88

6. Egert, P. Maliska, A.M. Silva, H.R.T. Speller, C.V. 1999. *Surf. Coat.Technol.* **121** : 33-38

7. Poirier, D.R. and Geiger, G.H. 1994. *Transport Phenomena in Materials Processing*. Warrendale, Pa : Minerals, Metals & Materials Society : 491-493.